Haptic Rendering of Arthroscopic Meniscus Examination in SOFA

Øystein Bjelland[*†], Bismi Rasheed[*], and Andreas F. Dalen [†]
[*] *Cyber-Physical Systems Lab, Department of ICT and Natural Sciences, NTNU,* Ålesund, Norway
[†] *Aalesund Biomechanics Lab, Department of Research and Innovation, Møre and Romsdal Hospital Trust,* Ålesund, Norway
Email: oystein.bjelland; bismi.rasheed@ntnu.no, andreas.fagerhaug.dalen@helse-mr.no

***Abstract*—Learning to distinguish between healthy and degenerative meniscus tissue is an important skill for orthopedic surgeons, as it could impact further treatment. Virtual simulations with kinesthetic haptic feedback offers a safe way of practicing this skill. This study demonstrates reality-based haptic rendering of arthroscopic meniscus examination using Simulation Open Framework Architecture (SOFA). Indentation elastic modulus and Poisson's ratio was determined from biomechanical indentation tests on cadaveric meniscus specimens, and used in a real-time corotational finite element simulation with haptic feedback. The resulting contact force signal from the simulation was validated against experimentally obtained contact forces from probing on a cadaveric meniscus specimen. The simulation contact force signals in the normal direction were in well agreement with experimental data, with an average force of -4.16 N for the simulation, and -4.0 N for the experiment. The achieved refresh rate for the physics thread in the arthroscopic examination simulation scene was 25 Hz during contact, which is sufficient for real-time applications.**

***Index Terms*—Force Feedback; Haptic Feedback; Arthroscopy; Biomechanics; Surgical simulation**

I. Background

The paradigm shift in surgical training, with an increasing focus on simulation, drives the need for better surgical simulators [1], [2]. The importance of simulators for arthroscopic surgery have been highlighted as a means of providing safe training for surgeries without the risk of causing harm to the patient [3]. For suspected meniscus injuries, an arthroscopic examination is normally performed to assess the properties of the meniscus tissue. It has been shown that a decrease in the compressive modulus of the meniscus can be associated with degenerative tissue. For example showed Fischenich et al. a 41% decrease in equilibrium modulus of the posterior lateral meniscus going from arthrosis grade 0 to grade 2 [4]. Because a degenerative meniscus can lead to development of arthrosis, it will affect the treatment, such as the decision of whether to suture or resect a meniscal tear. Therefore, it is important for novice surgeons to learn to distinguish between healthy and degraded meniscus tissue during arthroscopic probing.

In virtual surgical simulation, kinesthetic haptic feedback enables training of muscle memory and fine motor movements required in surgery. A review assessed the value of haptic feedback in surgical simulators, and found that haptic feedback leads to a shorter learning curve, and that haptic feedback is considered more important than visual feedback [5]. For evaluating haptic feedback of maneuvers where the surgeon relies on tactile sensation, such as arthroscopic meniscus palpation, a reference force signal is often used. The concept of recording and modelling mechanical interactions with the purpose of providing haptic feedback, has been introduced as "haptic camera" [6], "reality-based modelling" [7], and "haptography" [8]. In this paper, we adopt the term "reality-based modelling" for the recording and subsequent haptic rendering of surgical maneuvers.

Real-time virtual surgical simulation with user interaction through kinesthetic haptic feedback imposes two main requirements to the system. The first is that the physics thread should run at about 30 Hz to satisfy visual refresh rates. This can be challenging to achieve for large simulation models, as finite element simulations can be computationally expensive. Alternatively could mass-spring methods or position based dynamics be used to model physics, but at the sacrifice of accuracy [9]. The second requirement is that the haptic thread should run at more than 500 Hz for soft materials, and 1000 Hz for stiff materials [10]. The reason is partly because human cutaneous mechanoreceptors can sense frequencies up to 500 Hz, and partly because the stability of the haptic system is dependent on a high refresh rate [11], [12]. To address these requirements, Peterlik et al. [13] developed the multirate compliant mechanisms method, where haptic forces from contact between the instrument and virtual tissue are formulated in the physics thread, and resolved in the haptic thread. Simulation platforms such as the Simulation Open Framework Architecture (SOFA) utilizes this method to solve the linear constraint problem (LCP), and enable haptic feedback at real-time refresh rates.

The contribution of this study is to demonstrate reality-based haptic rendering for arthroscopic meniscus examination simulation, and validate the haptic force signals against experimental data. We structure this paper as follows. First, a simulation setup developed using SOFA is presented, with indentation elastic modulus obtained from biomechanical indentation experiments. Next, we compare the resulting haptic force signals against experimental data from arthroscopic meniscus examination on a cadaveric meniscus specimen that was included in the indentation tests. The results are then discussed and some concluding remarks are provided.

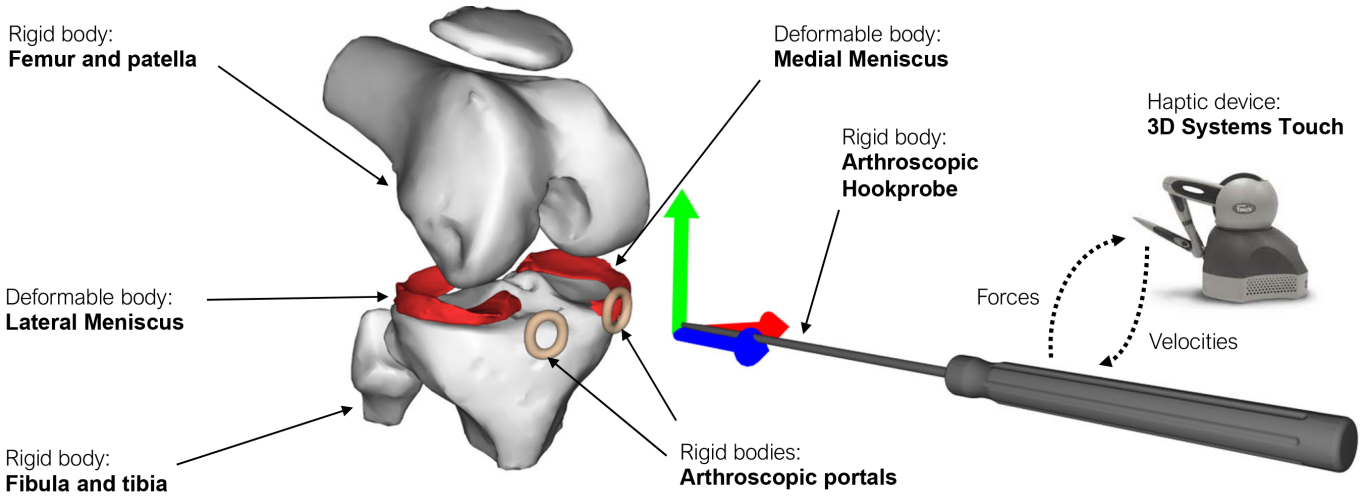

Fig. 1. An overview over the virtual 3D simulation models in the SOFA simulation scene. The lateral and medial mensci are modeled as deformable bodies, while the remaing models are rigid objects. The knee joint is modelled with a flexion of about 90 degrees to replicate surgical conditions. The arthroscopic hookprobe is controlled by a haptic device, and haptic feedback is transmitted back to the user. The refresh rate is about 25 Hz during probe-meniscus contact.

II. SOFA Simulation Setup

A. Simulation Models

The virtual simulation model consists of anatomical models of the femur, patella, fibula and tibia bones, as well as the lateral and medial menisci. The models were established from automatically segmented magnetic resonance imaging (MRI) knee models [14]. The lateral and medial portals were modeled as rigid body toruses. A computer aided design (CAD) model was developed of an arthroscopic hookprobe (type Arthrex AR 10000) using Siemens NX (Siemens, Germany) and imported into SOFA. An overview is shown in Fig. 1.

In SOFA, each virtual model can consist of independent visual-, collision- and computation models [15]. This allows for having a course finite element mesh that the reduce computation loads, and a finer resolution visual model that maintains visual realism. For the menisci models, the MRI-models were used directly as visual models, while the computation models were modelled using the X-form function in Siemens NX using the MRI-models as a template, and subsequently meshed with tetrahedral elements using G-mesh [16]. An illustration is shown in Fig. 2. Development of 3D tetrahedral mesh models directly from 2D surface models can be challenging because of fine details in the surface models. Creating the computation mesh from an isogeometric CAD model allows for better control of element size and distribution. The remaining virtual geometry were modeled as rigid bodies, and the same collision and visual models were used. The final simulation model is shown in Fig. 3.

B. Simulation Physics

The simulation scene was written in Python, interfacing SOFA using the SofaPython3 plugin. It consisted of a root node, the virtual model nodes, and a class accessing the contact forces between the virtual probe and meniscus models. An implicit Euler time integration scheme was used. The root node

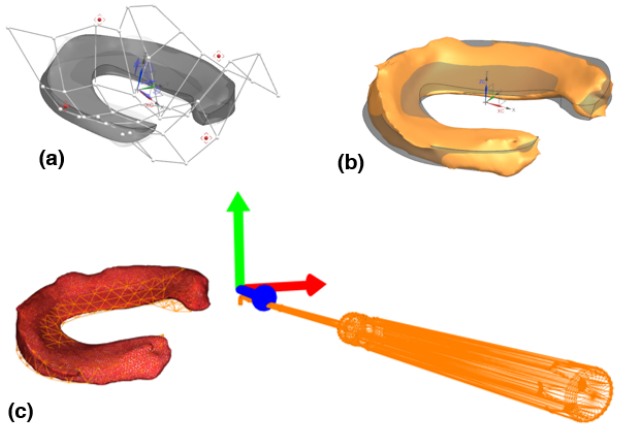

Fig. 2. Developing computation models of the menisci. (a) The X-form function in Siemens NX allows for subdividing surfaces and tracing anatomical models by "pulling nodes". (b) An overlay of CAD model and MRI model. (c) The computation and visual model of the lateral meniscus in SOFA.

included a 'FreeMotionAnimationLoop', and collision detection through the 'DefaultContactManager' with response set to 'FrictionContactConstraint'. The 'FreeMotionAnimationLoop' handles collision between objects by (i) computing the free motion with no constraint, (ii) perform collision detection, (iii) solve collision constraints by solving Langrange multipliers (λ), and (iv) apply the the corrected motion to the deformable objects. The deformable menisci (lateral and medial) were modeled as linear elastic corotational finite element models. A corotational finite element model was selected as it allows for modelling large deformations while maintaining a linear elastic material model. The menisci nodes therefore included an Euler implicit solver for time integration, a Conjugate Gradient linear solver, and precomputed constraint correction. Barycentric mapping was used for linking the visual and computation

models.

For haptic feedback, a 3D systems Touch haptic device (3D Systems, USA), formerly known as Geomagic Touch, was used. The Geomagic plugin, and 'GeomagicDriver' was therefore added to the root node, along with the 'LCPContraintSolver'. The LCPConstraintSolver solves for unilateral constraints, which corresponds to contacts with friction between objects. In the arthroscopic hookprobe node, 'LinearSolverConstraintCorrection' was added to compute the compliance of the contact. Further, the haptic device proxy and virtual arthroscopic hookprobe were connected using a 'RestShapeSpringsForceField', providing spring coupling to satisfy stability [12].

To access contact forces between the virtual arthroscopic hookprobe and meniscus for validation purposes, a class was written in python. The SofaPython3 plugin exposes the c++ components available in SOFA to Python, enabling extraction of constraint forces and directions from the linear constraint problem (LCP). Because the constraint forces, λ, are formulated in constraint space in SOFA [13], they must be transformed from constraint space to the cartesian world space with the following transformation:

$$\lambda(x, y, z) = \frac{H^T \lambda(n, t_1, t_2)}{dt}, \tag{1}$$

where $\lambda(x, y, z)$ are the contact forces in world space, dt is the time step, H is the constraint Jacobian, and $\lambda(n, t_1, t_2)$ are the contact forces in constraint space. The constraint Jacobian was extracted from the meniscus 'mechanical object', and the constraint forces were retrieved from the 'LCPConstraintSolver'. The transformation was computed while there was contact between the arthroscopic hookprobe and meniscus, and the output was saved to a comma separated value (CSV) file.

C. Material Constants

In another study, we have conducted biomechanical indentation tests and subsequent inverse parameter identification to obtain the indentation elastic modulus and Poisson's ratios on meniscus specimens from five cadaveric knees [17]. The average elastic modulus was found to be 3.50 MPa for the lateral meniscus, and 3.84 MPa for the medial meniscus. Although the meniscus could be modelled with region-wise differences, and as anisotropic and hyperelastic, we use a linear-elastic formulation to reduce computation loads and meet real-time requirements. The average values of the Poisson's ratios were found to be 0.29 for the lateral meniscus, and 0.26 for the medial meniscus.

III. Experimental Comparison of Contact Forces

A. Motivation

To evaluate the accuracy of haptic contact forces calculated in SOFA, we study contact forces during probing of the lateral meniscus. The resulting force signals are compared against experimentally obtained contact forces during examination of a cadaveric meniscus specimen. The cadaveric specimen was previously included in biomechanical indentation tests with inverse parameter identification to obtain the indentation elastic modulus and Poisson's ratio described in II-C, and is therefore representative for the given material properties [17].

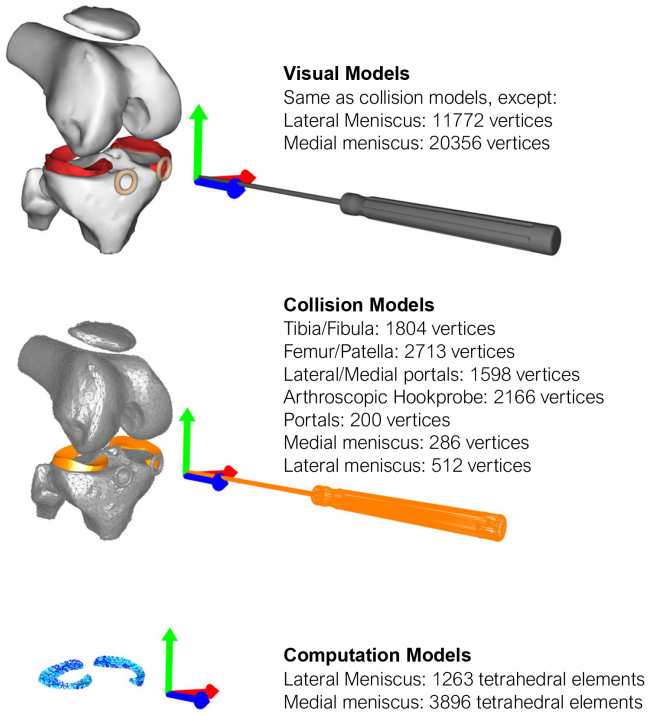

Fig. 3. Model representations in SOFA. Each model consists of a visual, collision and simulation model.

B. Method

1) Meniscus Experiment: An uninjured lateral meniscus specimen was obtained (Science Care, USA). The research was approved by the Regional Ethics Committee under reference 214114. The specimen was stored in a freezer at -28^oC and was thawed at room temperature for 5 hours before the experiment.

An arthroscopic probe equipped with an ATI Nano25 force/torque sensor (ATI Industrial Automation, USA), a ZED Mini stereo camera with an inertial measurement unit (IMU), was used to measure interaction forces between the arthroscopic probe and meniscus tissue, as well as the probe pose. The implementation is described in detail in [18].

The meniscus specimen was placed in a 3D-printed jig with an asymmetric v-groove for support. The groove was coated with sandpaper to prevent the meniscus specimen from slipping. The examination protocol was five probings in the posterior, mid and anterior regions of the lateral meniscus. The force and pose signals were recorded and saved to a CSV-file. The sampling rate was approximately 38 Hz.

2) SOFA Simulation: In SOFA, a scene consisting of only the lateral meniscus was created as described in II. A fixed boundary condition was applied to the nodes on the inferior surface of the lateral meniscus simulation model. The simulation was run on a laptop with 11th Gen Intel Core i5-11300H @ 3.10 GHz CPU, and 8 GB memory.

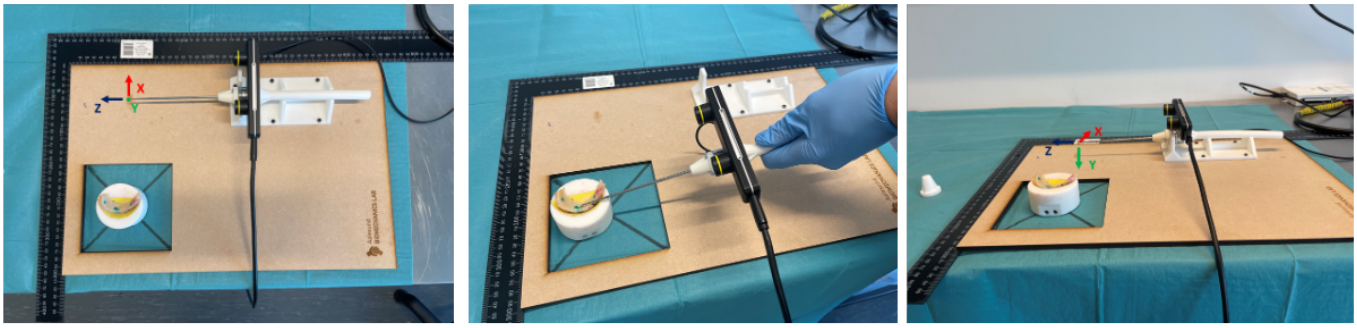

Fig. 4. The experimental setup for performing meniscus examination using the arthroscopic tracker probe.

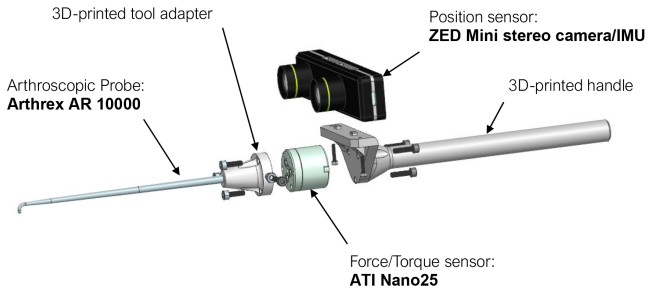

Fig. 5. The main components of the arthroscopic tracker probe, as described in detail in [18].

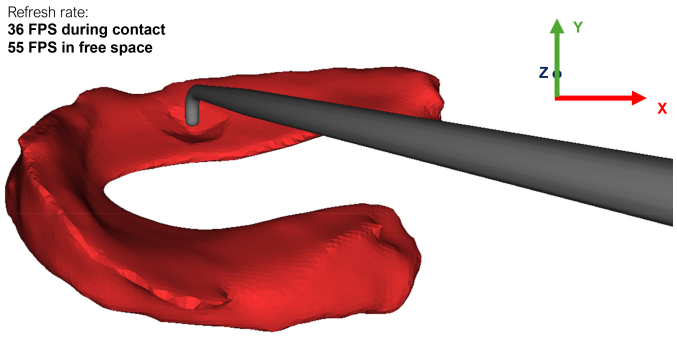

Fig. 6. Screengrab of interaction between probe and meniscus tissue in SOFA. The refresh rate during contact is 36 FPS, and 55 FPS when the probe moves in free space.

C. Results

Fig. 7 shows a descriptive comparison between the measured experimental contact forces, and the contact forces obtained from the SOFA simulation. The magnitude of the simulation force signal was in well agreement with the experimental data. In the Y-direction, the mean force during contact was -4.0 N for the experimental data, and -4.16 N for the simulation data. The direction of the force signals in Y-direction (green plot), which was the primary direction of contact, showed the same profile. The force signals in X and Z directions exhibited some minor differences, but the order of magnitude was consistent. The maximum displacement of the virtual instrument in Y-direction during probing was 7.7 mm.

IV. Discussion

This study has demonstrated haptic rendering of probe-tissue interaction during meniscus examination of a healthy meniscus, and validated the simulation against experimental force data. The force signals of the simulation were in well agreement with the experimental force signals. The corresponding displacement of the virtual instrument in Y-direction was 7.7 mm, which is higher than expected compared to indentation tests in [17], which utilized a probe displacement of 1 mm.

The large displacement could possibly be explained by the assumption of linear elasticity, as the nonlinear hardening effect is not considered. Also, boundary conditions and mesh size could affect the displacement. Because only the nodes of the inferior surface was constrained, as opposed to the entire surface, the coarse mesh allowed pieces of the tissue deform between the nodes. Detailed contact between the inferior surface of the lateral meniscus and tibial plateau would mitigate this issue. Other studies have also showed that the tissue stiffness is dependent on the mesh size [19]. This is a trade-off that must be balanced to meet real-time constraints.

From Fig. 7 the simulation contact forces in X and Z directions exhibited direction that deviated from the experimental results. This could partly be explained by the meniscus specimen not being horizontal in the experimental setup. The other reason could be because the forces in X and Z directions are primarily dominated by tangential contributions, essentially friction, which is even more sensitive to the user input movement than normal forces. In the simulation, the mesh size will also influence this behavior.

The mass of the end effector of the haptic device could also influence the contact forces. A steady state contact where the probe was at rest against the meniscus tissue produced about 1.4-1.6 N of contact force depending on how the haptic stylus was gripped. With the virtual instrument mass of 35 g, one would expect a contact force at steady state to be about 0.35 N if the haptic device was completely transparent. Effectively capturing the dynamic transfer function of the haptic device and use this to mask the inertia of the haptic device, such as demonstrated in recent work by Fazlollahi and Kuchenbecker [20], could be used to improve accuracy.

Considering clinical relevance, this study has demonstrated

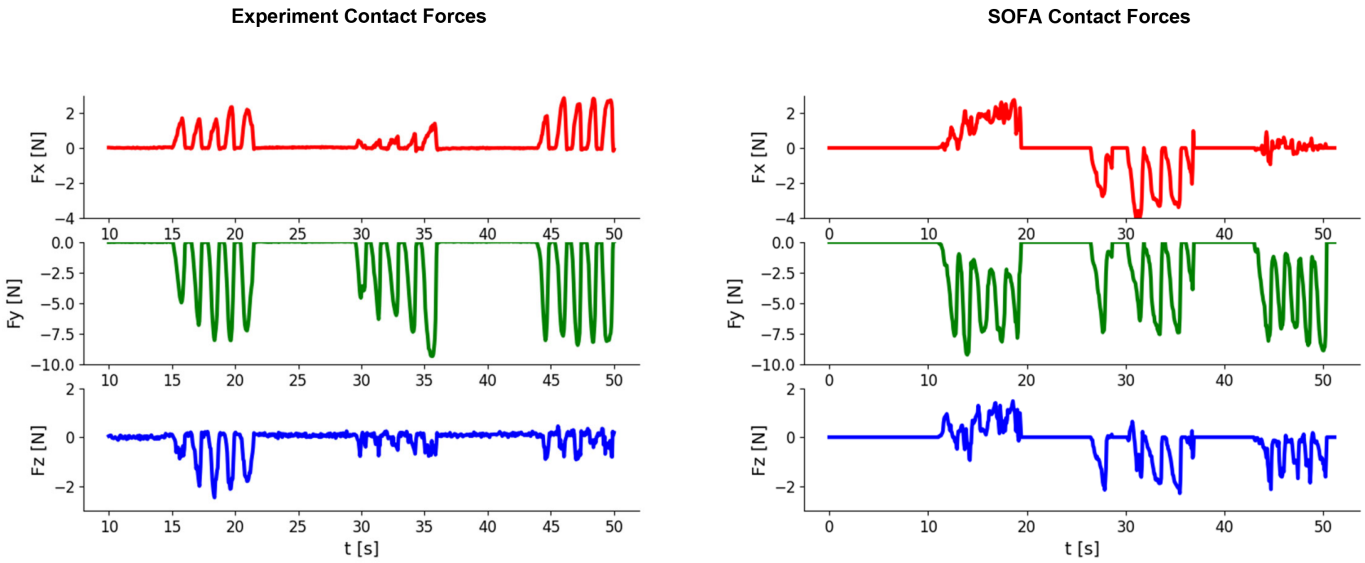

Fig. 7. Left: The plots show the resulting forces in the x, y and z directions from the experiment probing. Right: The resulting contact forces from SOFA simulation following the same protocol. The magnitude of the force signals are in well agreement.

haptic modelling of meniscus examination of a healthy meniscus for training purposes. To model different levels of meniscus degeneration, we propose to use material properties from healthy tissue as a base line, and scale the indentation elastic modulus according to the modulus decrease presented by Fischenich et al. [4]. A validation of the haptic rendering capabilities of the virtual simulator for the different nuances of degenerative meniscus tissue should be investigated in future studies.

V. Concluding Remarks

This study has demonstrated reality-based haptic rendering of arthroscopic meniscus examination using Simulation Open Framework Architecture (SOFA). Indentation elastic modulus and Poisson's ratio from biomechanical indentation tests with inverse parameter identification was used for interactive simulation. The resulting contact force signals from the real-time simulation was validated against experimentally obtained contact forces from a cadaveric meniscus specimen. The magnitude of the force signals were in agreement. More work is needed to validate haptic rendering capabilities of the simulator in terms of various levels of degenerative meniscus tissue.

Acknowledgement

The authors would like to acknowledge Kjell-Inge Gjesdal and Carl Petter Kulseng at Sunnmøre MR-Klinikk for providing the MRI-based anatomical models used in this project. The authors would also like to thank Hugo Talbot at the SOFA consortium for help with retrieving the contact simulation forces.

Ethical Declaration

This work has been considered by the Regional Ethics Committee under reference 214114. This study has followed the ethical principles for medical research involving human subjects outlined in the Declaration of Helsinki.

References

[1] N. Berte and C. Perrenot, "Surgical apprenticeship in the era of simulation," *Journal of Visceral Surgery*, vol. 157, no. 3, Supplement 2, pp. S93–S99, Jun. 2020.

[2] J. Lu, R. F. Cuff, and M. A. Mansour, "Simulation in surgical education," *The American Journal of Surgery*, vol. 221, no. 3, pp. 509–514, Mar. 2021.

[3] R. M. Frank, "Editorial Commentary: Arthroscopic Simulators—Are We There Yet?" *Arthroscopy: The Journal of Arthroscopic & Related Surgery*, vol. 35, no. 8, pp. 2391–2393, Aug. 2019.

[4] K. M. Fischenich, J. Lewis, K. A. Kindsfater, T. S. Bailey, and T. L. Haut Donahue, "Effects of degeneration on the compressive and tensile properties of human meniscus," *Journal of Biomechanics*, vol. 48, no. 8, pp. 1407–1411, Jun. 2015.

[5] E. M. Overtoom, T. Horeman, F.-W. Jansen, J. Dankelman, and H. W. R. Schreuder, "Haptic Feedback, Force Feedback, and Force-Sensing in Simulation Training for Laparoscopy: A Systematic Overview," *Journal of Surgical Education*, vol. 76, no. 1, pp. 242–261, Jan. 2019.

[6] K. E. MacLean, "The haptic camera: A technique for characterizing and playing back haptic properties of real environments," *Proc. of Haptic Interfaces for Virtual Environments and Teleoperator Systems (HAPTICS)*, pp. 459–467, Nov. 1996.

[7] A. Okamura, M. Cutkosky, and J. Dennerlein, "Reality-based models for vibration feedback in virtual environments," *IEEE/ASME Transactions on Mechatronics*, vol. 6, no. 3, pp. 245–252, Sep. 2001.

[8] K. J. Kuchenbecker, "Haptography: Capturing the Feel of Real Objects to Enable Authentic Haptic Rendering (Invited Paper)," in *Proceedings of the First International Conference on Ambient Media and Systems*. Quebec, Canada: ICST, 2008.

[9] Ø. Bjelland, B. Rasheed, H. G. Schaathun, M. D. Pedersen, M. Steinert, A. I. Hellevik, and R. T. Bye, "Toward a digital twin for arthroscopic knee surgery: A systematic review," *IEEE Access*, vol. 10, pp. 45 029–45 052, 2022.

[10] B. Hannaford and A. M. Okamura, "Haptics," in *Springer Handbook of Robotics*, B. Siciliano and O. Khatib, Eds. Berlin, Heidelberg: Springer, 2008, pp. 719–739.

[11] J. C. Makous, R. M. Friedman, and C. J. Vierck, "A critical band filter in touch," *Journal of Neuroscience*, vol. 15, no. 4, pp. 2808–2818, Apr. 1995.

[12] J. Colgate, M. Stanley, and J. Brown, "Issues in the haptic display of tool use," in *Proceedings 1995 IEEE/RSJ International Conference on Intelligent Robots and Systems. Human Robot Interaction and Cooperative Robots*, vol. 3, Aug. 1995, pp. 140–145.

[13] I. Peterlik, M. Nouicer, C. Duriez, S. Cotin, and A. Kheddar, "Constraint-Based Haptic Rendering of Multirate Compliant Mechanisms," *IEEE Transactions on Haptics*, vol. 4, no. 3, pp. 175–187, Jul. 2011.

[14] C. P. S. Kulseng, V. Nainamalai, E. Grøvik, J.-T. Geitung, A. Årøen, and K.-I. Gjesdal, "Automatic segmentation of human knee anatomy by a convolutional neural network applying a 3D MRI protocol," *BMC Musculoskeletal Disorders*, vol. 24, no. 1, Jan. 2023.

[15] F. Faure, C. Duriez, H. Delingette, J. Allard, B. Gilles, S. Marchesseau, H. Talbot, H. Courtecuisse, G. Bousquet, I. Peterlik *et al.*, "Sofa: A multi-model framework for interactive physical simulation," in *Soft tissue biomechanical modeling for computer assisted surgery*. Springer, 2012, pp. 283–321.

[16] C. Geuzaine and J.-F. Remacle, "A three-dimensional finite element mesh generator with built-in pre-and post-processing facilities," *Int. J. Numer. Methods Eng*, vol. 11, p. 79, 2009.

[17] B. Rasheed, O. Bjelland, A. F. Dalen, U. A. Schaarschmidt, H. G. Schaathun, M. D. Pedersen, M. Steinert, and R. T. Bye, "Intraoperative identification of patient-specific elastic modulus of the meniscus during arthroscopy," *in review*, 2024.

[18] Ø. Bjelland, L. I. Hatledal, R. T. Bye, and M. Steinert, "Implementation and Evaluation of an Arthroscopic Tracker System for Intraoperative Motion Tracking and Force Registration," in *Proceedings of the 37th ECMS International Conference on Modelling and Simulation*. ECMS, Jun. 2023, pp. 459–465.

[19] N. Schulmann, S. Cotin, and I. Peterlik, "The Effect of Discretization on Parameter Identification. Application to Patient-Specific Simulations," in *Computer Methods, Imaging and Visualization in Biomechanics and Biomedical Engineering*, 2020.

[20] F. Fazlollahi and K. J. Kuchenbecker, "Haptify: A measurement-based benchmarking system for grounded force-feedback devices," *IEEE Transactions on Robotics*, vol. 39, no. 2, pp. 1622–1636, 2023.